Journal of Power Sources 195 (2010) 3900–3906

Contents lists available at ScienceDirect

Journal of Power Sources

journal homepage: www.elsevier.com/locate/jpowsour

Thermodynamic measurements pertaining to the hysteretic intercalation of lithium in polymer-derived silicon oxycarbide

Dongjoon Ahn[1], Rishi Raj*,[1]

Department of Mechanical Engineering, University of Colorado at Boulder, Engineering Center, Colorado Blvd Boulder, Boulder, CO, 80309-0427, United States

ARTICLE INFO

Article history:
Received 16 December 2009
Received in revised form
19 December 2009
Accepted 22 December 2009
Available online 14 January 2010

Keywords:
Silicon oxycarbide
Anodes
Lithium ion batteries
Electrochemical measurements

ABSTRACT

Silicon oxycarbide (SiCO), made from the polymer route from siloxane-based precursors, has impressive capacity for serving as anodes in Li^+ batteries. However, the voltage–charge cycle exhibits significant hysteresis: the magnitude of the insertion voltages is low, while the extraction voltages are high. Here, we present coulometric titration results on both traverses of the cycle that lead to a measurement of an intrinsic polarization within the half-cell. This polarization-potential, which is measured to be 250–500 mV, is attributed to a differential between the potential of Li ions across the anode–electrolyte interface. In the second set of experiments the polarization was measured after coating the powders of the active anode material with a few monolayers of alumina by atomic-layer deposition (ALD). These results showed a shift of the hysteresis curve by ~50 mV, which is attributed to a space–charge double layer, most likely at the alumina–electrolyte interface. In the third result, the distribution of the "density of states" at different voltage levels where Li is inserted, and extracted, from SiCO is measured. The distribution is broad reflecting the amorphous nature of SiCO, and consistent with the strongly sloping behavior of the voltage–charge capacity profile of the charge–discharge cycle.

1. Introduction

Polymer-derived ceramics, or PDCs, are a new class of materials which myriad properties [1] that apparently arise from the graphene nanodomains [2] and the mixed bonds between silicon, carbon, oxygen and nitrogen that form when siloxane and silazane based polymers are pyrolyzed. During pyrolysis the hydrogen atoms become dissociated from the alkyl groups present in the organic state leading to the evolution of the nanodomain structure [3]. The most remarkable feature of the PDCs is the thermodynamic stability of their amorphous structure [4], and their zero creep behavior at temperatures as high as 1500 °C [5–7]. More recent work has revealed that the PDCs also have interesting functional properties such as photoluminescence [8–10], electronic conductivity [11] that extends into high temperature semiconductivity [12], and giant gage factors for piezoresistivity, not only at room temperature [13] but also at high temperatures [14].

Yet another property of the PDCs is their ability to store lithium at potentials such that they could be viable anode materials for Li^+ batteries. These data [15] were analyzed recently in terms of the nanodomain model of the PDCs [2]. The high capacity of these siloxane-derived ceramics was attributed to the mixed coordination between silicon, carbon and oxygen [16]. The influence of substituting oxygen, partially, with nitrogen on the lithium capacity has also been studied [17], leading to the conclusion that the capacity is reduced if the molar ratio of nitrogen to oxygen is greater than unity, but not otherwise.

The lithium capacity of the PDCs is two, or even three times larger than graphite. Measurements from a half-cell (measured with lithium metal as the counter electrode), given in Fig. 1, show a total capacity of 1164 mAh g^{-1}, and a reversible capacity of 794 mAh g^{-1}; the coulombic efficiency for the first cycle is 68.2%. The insertion–extraction cycle, however, exhibits significant hysteresis; the differential between the Li-insertion and Li-extraction voltage can approach 1 V (one volt). If the experiment is carried out "reversibly", i.e. near equilibrium at very slow charge–discharge rates, then the extent of hysteresis should narrow, and in the limit, vanish if there are no intrinsic polarizations within the system. One objective of this work was to measure these thermodynamic potentials during insertion and extraction, to check whether or not they converge to the ideal Nernst potential for lithium intercalation into the PDCs. These potentials are accessible by coulometric titration.[2]

* Corresponding author. Tel.: +1 303 492 1029; fax: +1 303 492 3498.
E-mail address: rishi.raj@colorado.edu (R. Raj).
[1] Both the authors are affiliated with PDC-Energy, LLC, Louisville, CO 80027-3605, USA.

[2] Coulometric titration is a general name for measuring the change in potential in an electrochemical cell at constant current, or conversely measuring the current at a given applied potential. The current experiments do not adhere to these procedures, instead we measure the change in the potential at zero current after injected a given

0378-7753/$ – see front matter © 2010 Elsevier B.V. All rights reserved.
doi:10.1016/j.jpowsour.2009.12.116

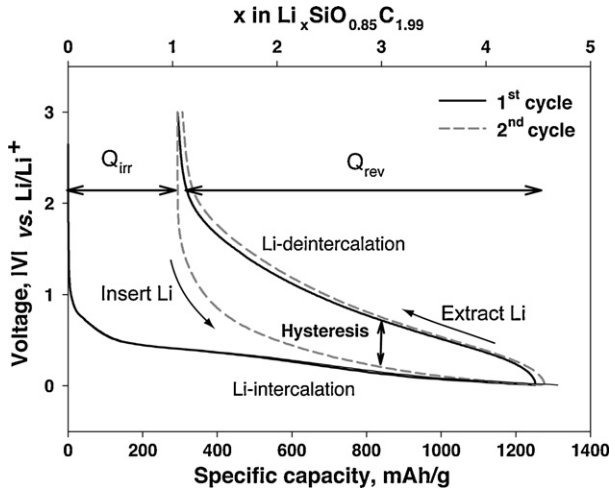

Fig. 1. The insertion and extraction of lithium into polymer-derived SiCO is hysteretic.

We shall find that the equilibrium potential, for the same state of charge, is different for the two halves of the cycle, reflecting an intrinsic polarization within the half-cell. Furthermore, the influence of a few monolayers of alumina coating on the PDC particles on this intrinsic polarization is measured, which provides further insights into interfacial polarization and space–charge layers at the anode–electrolyte interface.

Another feature of the voltage–charge cycles shown in Fig. 1, is the continuously sloping behavior of the voltage locus, which suggests that the presence of a broad band of energy levels for the insertion of lithium. This density of states (DOS) distribution, that is, the capacity of lithium at different energy levels, is measured by extracting the charge from the anode material[3] in stepwise increments in the applied voltage. The DOS diagram, exhibits a broad distribution, resembling log-normal behavior with a peak at approximately 0.1 V during insertion and 0.6 V during extraction.

(The terminology of DOS is commonly used to describe the energy levels that are available to be occupied by electrons in the field of solid-state physics. However, intrinsically, the DOS is a distribution of energy levels, relative to a reference, which describes the maximum number of a given species that can occupy these energy levels. In solid-state terminology these species are usually electrons; here the species are lithium. A specific energy level means the interaction energy, expressed as the Gibbs free energy, between a lithium atom and a certain molecular site in the material. The interaction energy is measured relative to pure lithium metal. The "density" is equal to the number of sites in the material having this specific value of the interaction energy. Therefore, the DOS for lithium interaction is the distribution of the number of sites available at different energy levels for lithium insertion. Note that the interaction energies are expressed as Gibbs free energy—they are to be converted to voltage by dividing by the Faraday's constant.).

The experiments were carried out with anodes made from powders of siloxane-derived ceramics. Carbon-black was used as the conducting agent to facilitate a nearly equal electron electrochemical potential between the surfaces of the anode particles, and

charge into the anode material, corresponding to one half of GITT (Galvanostatic intermittent Titration Technique) cycle [18].

[3] We use the term anode and PDC (as a material with properties related to lithium intercalation) interchangeably in this paper, recognizing well that, from an electrochemical point of view, the terminology for electrodes used in full cells does not apply to half–cells.

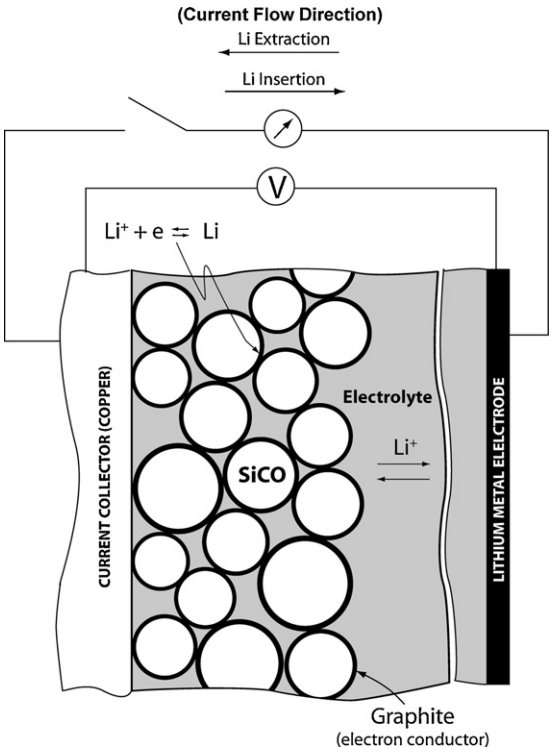

Fig. 2. The microstructure of the SiCO electrode used to measure its lithium intercalation properties.

copper, which serves as the current collector. This microstructure of the anode is illustrated schematically in Fig. 2.

2. Experimental

2.1. Synthesis of the anode powder

Polymer-derived silicon oxycarbide (SiCO) powders were synthesized by controlled pyrolysis of crosslinked organic polymers. 1,3,5,7-tetramethyl-1,3,5,7-tetravinylcyclotertrasiloxane (TTCS, Gelest, USA) was used as the precursor. 1 wt% dicumyl peroxide of the total amount of TTCS was added to promote cross-linking. The liquid precursor was crosslinked at 380 °C for 5 h in Ar purged furnace (Thermolyne, IA). The crosslinked polymer monolith was ball-milled for 1 h in plastic jar with zirconia balls as the grinding media. The milled powder was pyrolyzed at 1000 °C for 5 h under argon purged tubular furnace. Heating rates for cross-linking and pyrolysis were 90 °C h^{-1} and 240 °C h^{-1}, respectively. The cooling rates were the same as the heating rates. After full pyrolysis, a black ceramic powder was obtained.

Elemental analysis of the SiCO powder was done for its oxygen, and carbon content. Silicon content was calculated as the difference between the sum of the measured oxygen and carbon content and the total weight of the specimen. The carbon content was measured by combustion (LECO Corp., Model C-200) method with accelerants as iron chip and Lecocel II HP. The oxygen content was analyzed by fusion (LECO Corp., TC-600) method. Cast iron with 3.36% carbon was used as standard in carbon analysis and tungsten oxide was selected as the standards for oxygen analysis.

The composition of the powder was $SiC_{1.98}O_{0.85}$.

2.2. Atomic-layer deposition (ALD) of Al_2O_3 on SiCO

SiCO was coated with a few monolayers of Al_2O_3 by the ALD method. Recently, such treatment of electrode materials has

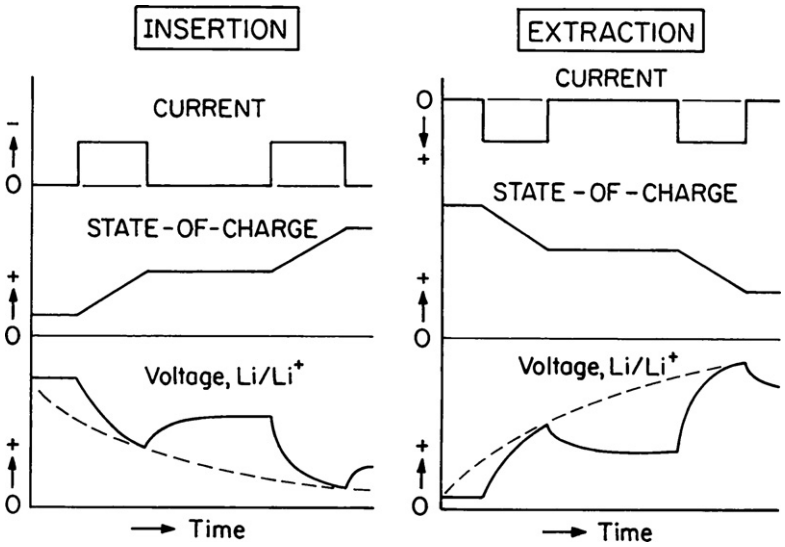

Fig. 3. Schematic of the experiments carried out to measure the equilibrium potentials at various states of charge during the insertion and extraction parts of the cycle.

attracted attention for enhancing the performance of electrode materials for lithium ion batteries [19]. The alumina coating by ALD in this present work [20] was done directly on the PDC anode, composed of PDC powder, acetylene black and polyvinylidene fluoride (PVDF). The monolayers of alumina were determined by repeating the deposition cycle, as described below. Two and eight monolayers of Al_2O_3 were deposited.

The ALD reaction sequence was constituted of twelve steps. Each sequence produced on monolayer of Al_2O_3. The sequence consisted of the following steps: (1) trimethylaluminum (TMA) dose to 1.0 torr → (2) TMA reaction time → (3) evacuation of the reaction products and excess TMA → (4) N_2 dose to 20.0 torr → (5) N_2 static time → (6) evacuation of N_2 and any entrained gases → (7) H_2O dose to 1.0 torr → (8) H_2O reaction time → (9) evacuation of reaction products and excess H_2O → (10) dose N_2 → (11) N_2 static time → (12) evacuation of N_2 and any entrained gases. All processing steps were conducted at 180 °C [20].

2.3. Half-cell preparation

The anode electrodes for the measurement of electrochemical properties were prepared by mixing a slurry consisting of 80 wt% of active material (SiCO), 10 wt% acetylene black, and 10 wt% of PVDF dissolved in 1-methyl-2-pyrrolidinone. The slurry mixture was screen printed on to a copper foil using a doctor blade and a film applicator. This electrode served as the working electrode in a CR 2032-type coin cell. A lithium foil was used as the counter and reference electrode, for a half-cell configuration. Microporous polypropylene (PP) (Celgard, USA) and 1 M LiPF6 in a mixed solution of ethylene carbonate and diethyl carbonate (volume ratio 1:1, Ferro Corporation, USA) were used as the separator and the electrolyte, respectively. The coin-cells were assembled, crimped and closed in an argon filled glove box. The electrochemical measurements were performed at lithium insertion and extraction current density of 100 mA g^{-1}, between voltage limits of 0.01 V and ~3 V.

2.4. The testing methods

2.4.1. Measurement of polarization

The objective of the first experiment was to measure the thermodynamic potential of Lithium in the anode at different states of charge, during insertion, and then during extraction. Charge was inserted (or withdrawn) at stepwise intervals at a constant current (100 mA g^{-1}). The current was intermittently switched off and the change in the potential with time during this off-period was measured. The magnitude of the potential (with respect to the lithium metal electrode) rose when the current was turned off, during the insertion half of the cycle, but fell during the extraction half of the cycle. The experimental procedure used in these experiments is illustrated schematically in Fig. 3. Note that the voltage moves in opposite directions during intercalation and de-intercalation during the off-periods: the reason is given in Fig. 4. During insertion the gradient of Li within the anode particle is opposite to that when lithium is being extracted. During the off-period the lithium concentration seeks to level out by diffusion, however the surface concentration, which is what is measured by means of the voltage, moves in opposite directions during insertion and extraction.

2.4.2. Measurement of the density of states

After full insertion of lithium, the anode is allowed to equilibrate in open-circuit. Then an extraction voltage is applied in incremental steps. The lithium is stored in the anode at different energy levels, as illustrated in Fig. 5. Consider for example applying, in the first step, a voltage V_1. The total charge extracted from the anode (equal to the integrated value of the current) at this voltage gives the charge

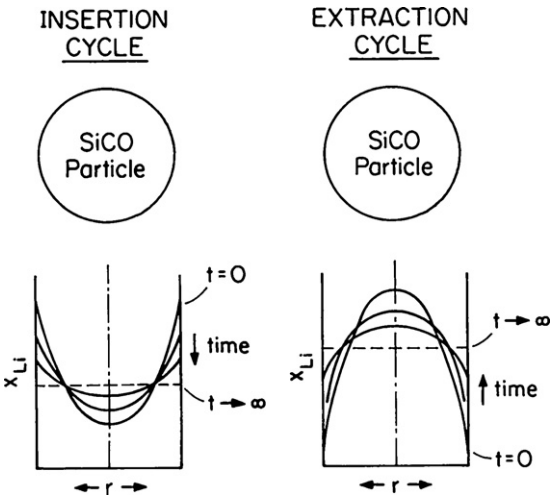

Fig. 4. The time dependent change in the profiles of lithium concentration in the SiCO particles during insertion and then during extraction. Note that the measured voltage corresponds to the surface potential.

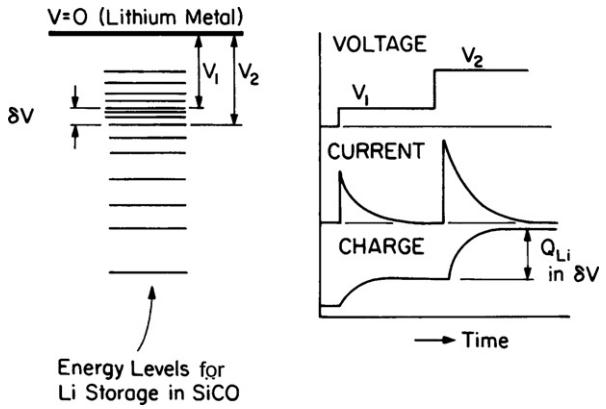

Fig. 5. Measurement of the density of states for lithium storage at various voltage levels within SiCO.

that can be stored at energy level $\leq V_1$. In the next step charge is extracted at V_2: this charge is stored at $V_1 \leq V \leq V_2$, and so on. In this way a histogram of the lithium charge stored at different energy levels is obtained.

3. Results

3.1. Thermodynamic potentials without ALD coatings

The full set of results is given in Fig. 6. The bottom of this figure gives the time dependent change in the open-circuit voltage at different states of charge (SOC). The SOC is defined as the charge of lithium contained in the anode expressed as a percentage of the maximum capacity of the anode. Each equilibration experiment was allowed to run for 24 h. The equilibrium values of the voltage obtained at different points along the charge–discharge curves are shown in the figure at top left: the loci for these points are drawn in dotted lines. The vertical spacing between the lines is the total polarization voltage which is shown on the top right at different states of charge: for example the voltage difference "*a*" is shown in the figure on the left and then, in the plot on the right.

These results have two noteworthy features. First, the equilibrium voltages from the charge and discharge cycles attempt to converge, which is consistent with a kinetic constraint on the cycle: that is if the cycle were to be performed infinitely slowly then the shape of the cycle would be that given by the dotted line in this figure. The second point is that a hysteresis deficit remains even under equilibrium conditions: this is discussed in terms of internal polarization in the next section.

3.2. Influence of ALD coatings on equilibrium potentials

Rather surprisingly we find that ALD coatings do not change the hysteresis behavior significantly. The results for two and eight monolayers are presented in Fig. 7. The principal effect is to shift the cycle slightly upwards to a higher voltage. The effect is not significantly dependent on the number of monolayers deposited on the anode particles. The shift is attributed to the development

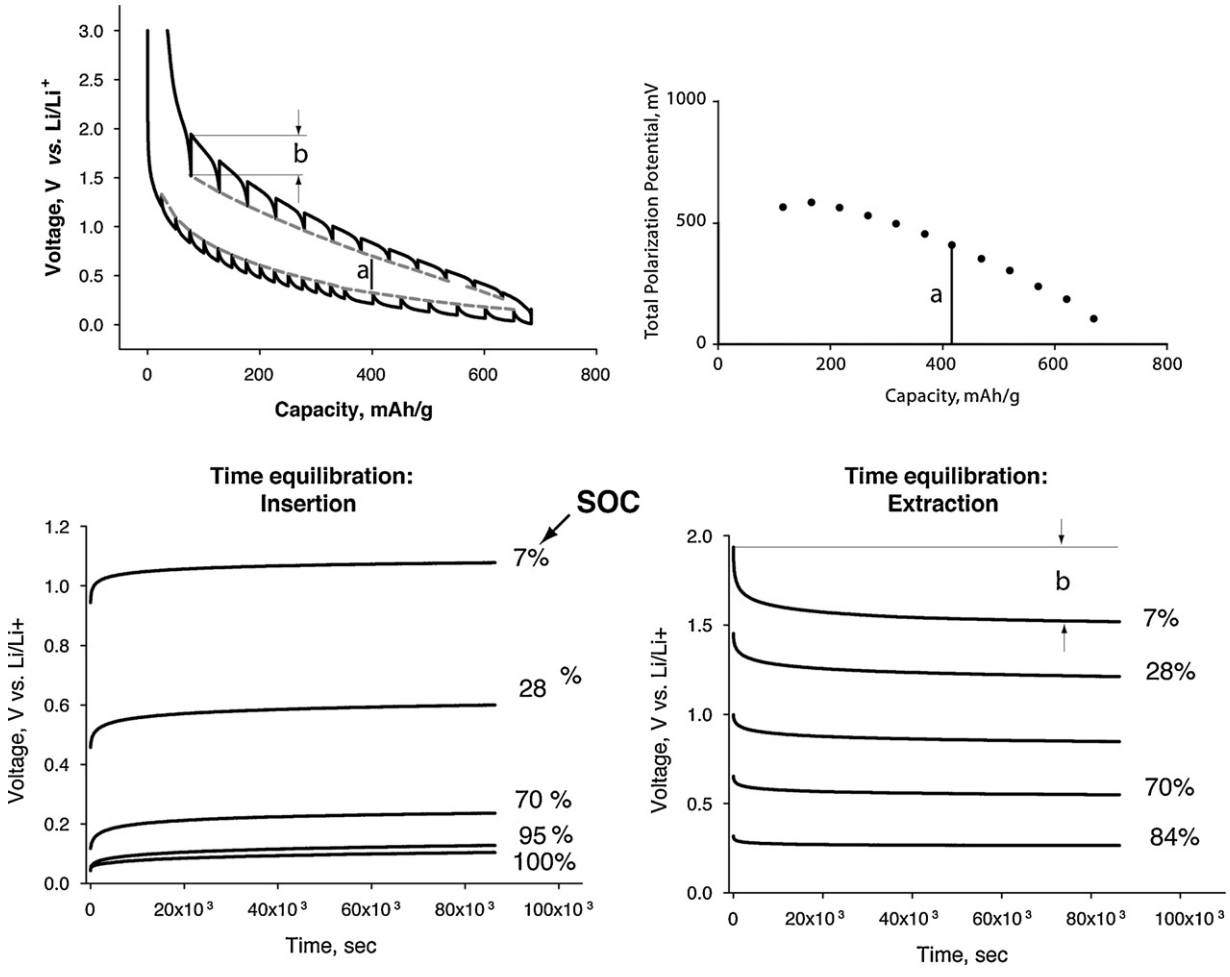

Fig. 6. Results for the equilibrium voltage of lithium during insertion and then during extraction halves of the cycle.

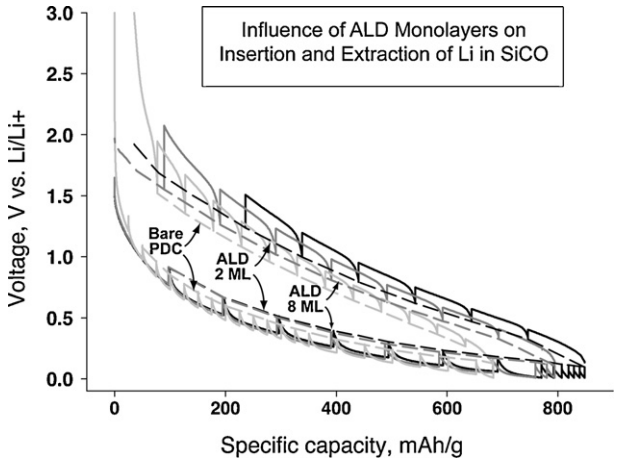

Fig. 7. Influence of two and eight monolayers of Al_2O_3 on the hysteresis behavior. The effect is shift of the curve in upwards direction.

of an internal voltage in the form of a space–charge layer; this is discussed further in the next section.

3.3. Measurement of the density of states

The density of states (DOS) was measured during the insertion as well as the extraction parts of the cycle. The results are given in Fig. 8. The difference in the data from the insertion and extraction halves of the cycle reflects the influence of internal polarization. Whereas the maximum insertion occurs at low voltages during insertion, it is shifted to approximately 0.5 V during extraction, a value that is similar to the height of the hysteresis shown in Fig. 1. This point is discussed in the next section.

4. Discussion

4.1. The hysteresis

The principal result in this work is the measurement of the equilibrium potentials achieved for PDC anodes at different states of charge (SOC), during lithium insertion and lithium extraction. (Strictly speaking a three-electrode system where the pure lithium potential is established with a reference electrode should be used for thermodynamic measurements. However, remanent polarization at the lithium metal electrode under open-circuit conditions is likely to have been negligible, since in similar experiments where the anode is made from graphite rather than from PDCs the voltage across the half-cell is about 10 mV much smaller than the values measured in the present experiments.) These potentials do not converge, as they should if the hysteresis arises solely from the kinetics of the charge–discharge cycle; if this were to be the case then the hysteresis would be reduced and eventually vanish when the charge and discharge are carried at even decreasing current densities. A similar finding has been reported for "hard carbon", where the hysteresis is attributed to an activation barrier for the extraction of lithium [21,22]. The explanation given here is along similar lines though different in detail: we shall argue that the hysteresis has thermodynamic, rather than a kinetic, origin.

Two features of the hysteresis are noteworthy. The first is that the hysteresis is asymmetric, that is, it occurs during the extraction half of the cycle. Experiments with different forms of carbon [21], which is consistent with our own experience, show that varying the chemistry of the anode materials affects hysteresis by moving the extraction half of the cycle: the insertion profile usually remains unchanged. The second observation is that the measurement of

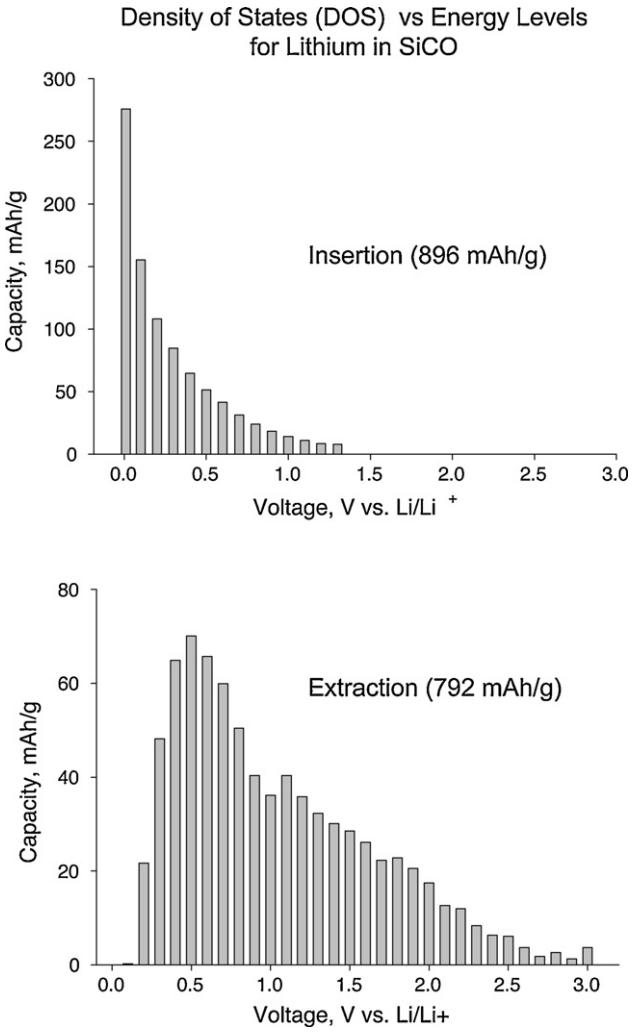

Fig. 8. The DOS for lithium intercalation into SiCO.

the DOS (Fig. 8) is asymmetric in the same sense as is the hysteresis, that is, the insertion voltages are lower than the extraction voltages.

The model that is presented below to explain the hysteresis depends on three assumptions: (i) at equilibrium, when the asymptotic value of the open-circuit voltage has been achieved, the chemical potential of Li^+ is uniform throughout the electrolyte, from the anode-interface to the lithium metal counter electrode: this is a reasonable assumption given the high mobility of Li^+ in the electrolyte. (ii) The ionization reaction of Li to Li^+ in the anode occurs at the interface between the SiCO particles and the electrolyte—this is justified because the SiCO material used in this study is essentially an insulator, so that the mobility of Li atoms in the PDC is far greater than the mobility of electrons. (iii) The hysteresis does not arise due to reactions at the electrolyte – Li metal interface – this is justified because half-cells constructed with graphite, with lithium metal counter electrodes do not exhibit hysteresis.

The assumptions above lead to the picture shown in Fig. 9. It includes the following "species": (i) Li atoms in the pure metal, written as Li^o, (ii) Li atoms in solution within the anode, Li_A, (iii) Li ions in the electrolyte, which are in equilibrium with pure lithium metal, Li^+, (iv) Li ions in the anode–electrolyte interface, which are denoted as Li_A^+, and (v) the electrons at the anode–electrolyte interface, which are simply written as "e" with the subscripts "o" for the metal electrode, and "A" for the anode. With this nomenclature, the following equations can be written to express equilibria between

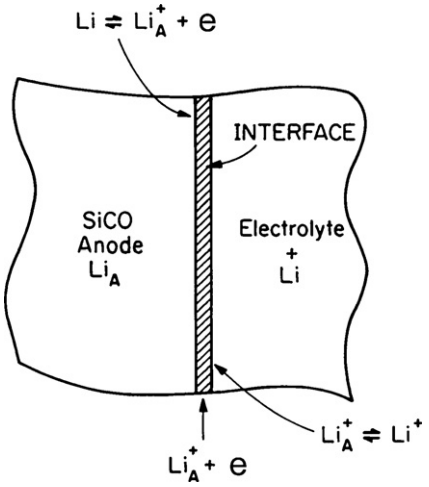

Fig. 9. The reactions at the SiCO–electrolyte interface.

the lithium metal and the ions and at the anode–electrolyte interface:

At the pure lithium metal:

$$\mathrm{Li^o} = \mathrm{Li^+} + \mathrm{e_o} \tag{1}$$

At the anode–electrolyte interface:

$$\mathrm{Li_A} = \mathrm{Li_A^+} + \mathrm{e_A} \tag{2}$$

Note that in the open-circuit condition the electron concentration in the anode becomes constant since the anode can no longer exchange with the counter electrode. Expressing the equilibrium in Eqs. (1) and (2) in terms of the electrochemical potentials of the species we have that:

$$\tilde{\eta}_{\mathrm{o}}^{\mathrm{Li}} = \tilde{\eta}_{\mathrm{Li^+}} + \mu_{\mathrm{e_o}} \tag{3}$$

and:

$$\tilde{\eta}_{\mathrm{Li_A}} = \tilde{\eta}_{\mathrm{Li_A^+}} + \mu_{\mathrm{e_A}} \tag{4}$$

Subtracting Eq. (3) from Eq. (4), and expressing the electrochemical potentials of the species in terms of their activities, described by a with the appropriate subscripts, we have that:

$$RT\ln a_{\mathrm{Li}}^{\mathrm{A}} = \Delta\tilde{\eta}_{\mathrm{Li_A^+}}^{\mathrm{Li^+}} - VF \tag{5}$$

where:

$$\Delta\tilde{\eta}_{\mathrm{Li_A^+}}^{\mathrm{Li^+}} = \tilde{\eta}_{\mathrm{Li_A^+}} - \tilde{\eta}_{\mathrm{Li^+}} \tag{6}$$

Here R is the gas constant, F is the Faraday's constant, and V is the open-circuit voltage. The sign of V is defined such that the PDC is at a positive voltage with respect to the lithium metal electrode.

The hysteresis may now be explained by considering the three possible cases of Eq. (5). The simple case occurs when $\tilde{\eta}_{\mathrm{Li_A^+}} = \tilde{\eta}_{\mathrm{Li^+}}$, when the measured voltage is related only to the activity of Li in the anode, that is, to the state of charge:

$$\bar{V} = \frac{-RT}{F}\ln a_{\mathrm{Li}}^{\mathrm{A}} \tag{7}$$

The bar on the voltage emphasizes that this case represents an effortless transfer of ions across the anode–electrolyte interface, in either direction. In this instance the open-circuit voltage measured during insertion and extraction cycles will be the same.

If on the other hand $\tilde{\eta}_{\mathrm{Li_A^+}} \neq \tilde{\eta}_{\mathrm{Li^+}}$, then the open-circuit voltage, given by the following equation, will be different from the case

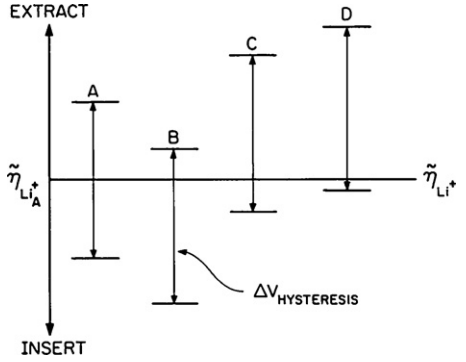

Fig. 10. The electrochemical potential of the lithium ions at the interface is expected to differ during insertion and extraction, giving rise to hysteresis.

described by Eq. (6):

$$V = \frac{-RT\ln a_{\mathrm{Li}}^{\mathrm{A}} + \Delta\tilde{\eta}_{\mathrm{Li_A^+}}^{\mathrm{Li^+}}}{F} \tag{8}$$

The result in Eq. (7) can predict the hysteresis if $\Delta\tilde{\eta}_{\mathrm{Li_A^+}}^{\mathrm{Li^+}}$ is unequal for the insertion and extraction halves of the cycle. Note that if $\tilde{\eta}_{\mathrm{Li_A^+}} < \tilde{\eta}_{\mathrm{Li^+}}$, then $V < \bar{V}$, and conversely if $\tilde{\eta}_{\mathrm{Li_A^+}} > \tilde{\eta}_{\mathrm{Li^+}}$, then $V > \bar{V}$. It immediately follows that hysteresis will occur if $[\tilde{\eta}_{\mathrm{Li_A^+}}]_{\mathrm{insert}} < \tilde{\eta}_{\mathrm{Li^+}}$ and $[\tilde{\eta}_{\mathrm{Li_A^+}}]_{\mathrm{extract}} > \tilde{\eta}_{\mathrm{Li^+}}$, keeping in mind that $\tilde{\eta}_{\mathrm{Li^+}}$ is fixed by the lithium metal electrode. In fact, in general, hysteresis is possible under various scenarios for the relative values of these three electrochemical potentials of lithium ion, as illustrated in Fig. 10. The case marked as "D" where the insertion voltage is close to equilibrium but the extraction voltage lies higher, is expected to apply to the present results.

The question arises how can it be possible that $\tilde{\eta}_{\mathrm{Li_A^+}} \neq \tilde{\eta}_{\mathrm{Li_A}}$, because the lithium ion in the electrolyte and in the PDC must equilibrate, bringing these two electrochemical potentials into unison. We believe this inequality to be thermodynamically rather than kinetically limited. Note in Fig. 2 that the hysteretic voltage difference persists even when the open-circuit voltage is allowed to reach equilibrium for 24 h, even though the asymptotic value of the voltage is nearly achieved in about 2 h.

A thermodynamic constraint to equilibration can arise, however, if the effective charge on the lithium ion in the anode is not the same as it is in the electrolyte. If this were the case then the transfer of ions across the interface (to achieve equilibrium) would require the transfer of electronic charge across the external circuit, which is not possible under open-circuit conditions. It may be argued, however, that charge balance can be established across the interface by exchanging, for example, two lithium ions in the interface which carry a charge of +0.5, with one ion in the electrolyte; such a scenario is likely to implausible because the probability of such an exact encounter at the interface would be very low.

4.2. The influence of ALD monolayers

The effect of depositing two (or eight) monolayers of aluminum oxide on the PDC particles is to shift the voltage–charge cycle slightly upwards by approximately 50–100 mV. In other words it moves the insertion and extraction curves in the same direction. Phenomenologically such a result can be expressed by adding a constant voltage, δV_{ALD}, to Eq. (7):

$$V = \frac{-RT\ln a_{\mathrm{Li}}^{\mathrm{A}} + \Delta\tilde{\eta}_{\mathrm{Li_A^+}}^{\mathrm{Li^+}}}{F} + \delta V_{\mathrm{ALD}} \tag{9}$$

Furthermore, the magnitude of δV_{ALD} is relatively insensitive to whether the thickness of the ALD is two or eight monolayers. This shift is attributed to an internal voltage developed by space–charge at the anode–electrolyte interface. Since the shift does not change significantly with the thickness of the ALD, the space–charge layer may be assumed to exist at the alumina–electrolyte interface (rather than the PDC–alumina interface), for the reasons outlined below.

(Recall that a space-charge is constituted from the segregation of a net charge to an interface, which is then balanced by a counter charge in the adjacent dielectric. It is necessary for the counter charges to be mobile in the dielectric so that they can form a profile to equilibrate the electrochemical potentials of the charged species across the space–charge layer. The effective width of this layer, also called the Debye layer depends on the dielectric constant of the medium containing the charged species, and on the concentration of the charged species in the dielectric.)

In the present problem the Debye layer is formed by the lithium ions. However, theoretically speaking, the dielectric medium can be either the alumina overlayers, or the electrolyte, or a combination of both (note that the lithium ions must have significant mobility in the alumina overlayers since the kinetics of charge–discharge is not significantly influenced by the ALD layers). However, if the alumina monolayers were participating in the construction of the Debye layer then they would have strongly influenced the space–charge voltage. Since that space–charge voltage is relatively unchanged by changing the thickness of the ALD by a factor of four, it is to be concluded that the electrolyte must have served as the principal medium for the Debye layer; a corollary inference is that interfacial charge of the double layer would have resided at the alumina–electrolyte interface.

4.3. The density of states

The polymer-derived SiCO, used as the anode in these experiments is an amorphous material, which is expected to have a nanodomain structure created by a network of graphene. In addition to sp^2 carbon, the structure also contains sp^3 silicon that is coordinated with oxygen and carbon atoms in different possible ways. These materials are made from the pyrolysis of highly crosslinked polysiloxanes. During pyrolysis hydrogen is lost from the alkyl groups of carbon, and these carbons, that are tethered mostly to silicon, are then assumed to self assemble into sp^2 carbon which is a strong feature of the PDCs. However, it is possible that some hydrogen is left behind in the ceramic (although measurements have shown the amount of this hydrogen to be extremely small [4]), which can influence the nature of lithium intercalation.

Therefore, the electronic structure of the PDCs is likely to be complex, offering a diversity of sites, with different binding energy for lithium. The results in Fig. 8 give the distribution of the density of states function for these sites. The distribution of the DOS is ostensibly different for the insertion and extraction parts of the cycle because of the hysteretic nature of this process, as has been discussed.

5. Conclusions

Measurements of the asymptotic values of the open-circuit voltage, at interrupted states of charge, provide insights into the basic reasons for the large hysteresis in silicon oxycarbide (SiCO) materials when used for lithium sequestration as anodes in lithium ion batteries. The persistence of hysteresis, albeit to a smaller extent, in these open-circuit voltage measurements suggests the hysteresis arises partly from the kinetics of lithium diffusion into the SiCO particles, and partly from thermodynamic limitations.

The present work provides possible insights into the origin of the thermodynamic portion of the hysteresis. It is attributed to a difference in the electrochemical potential of the lithium ions at the SiCO–electrolyte interface, and the electrochemical potential of the lithium ions within the electrolyte that are in equilibrium with the lithium metal counter electrode. It is proposed that these two electrochemical potentials are prevented from equalizing in the open-circuit condition because the effective charge on the lithium ions in the interface is different from the charge on lithium ions in the electrolyte. This is not an unreasonable expectation since the ionicity of the lithium bonding in the SiCO is likely to differ from that in the electrolyte.

The deposition of a few monolayers of alumina on the SiCO particles in the anode, produced by the ALD process, gave the unexpected result of producing an upwards shift in the voltage–charge cycle. Instead, we had expected that it would expand or contract the height of the hysteresis. The shift is attributed to the development of a space–charge layer at the alumina–electrolyte interface. The strength of this space-charge layer is in the 50–100 mV range.

Experiments were carried out to measure the charge stored in discrete voltage intervals at increasing and decreasing voltage levels. These results provide the density of state (DOS) diagram for lithium intercalation in the SiCO. The energy level diagram is quite broad, which is consistent with the amorphous nature of SiCO, and the construction of its molecular structure from different kinds of bonds, ranging from sp^2 carbon to silicon tetrahedra coordinated with carbon and oxygen atoms in different ways.

Acknowledgements

This research was supported by the Ceramic Program in the Division of Materials Research at the National Science Foundation under grant no: DMR-09-07108. We thank Professor Steven George for the ALD coatings on SiCO. We are grateful to Prof. SeHee Lee for introducing us to the field of electrochemistry, and especially to the experimental methods in electrochemistry.

References

[1] R. Raj, R. Riedel, G.D. Sorarù, J. Am. Ceram. Soc. 84 (2001) 2158–2159.
[2] A. Saha, D.L. Williamson, R. Raj, J. Am. Ceram. Soc. 89 (2006) 2188–2195.
[3] G.D. Soraru, L. Pederiva, J. Latornerie, R. Raj, J. Am. Ceram. Soc. 85 (2006) 2181–2187.
[4] T. Varga, A. Navrotsky, J.L. Moats, R.M. Morcos, F. Poli, K. Muller, A. Saha, R. Raj, J. Am. Ceram. Soc. 90 (2007) 3213–3219.
[5] L. An, R. Riedel, C. Konetschny, H.-J. Kleebe, R. Raj, J. Am. Ceram. Soc. 81 (1998) 1349–1352.
[6] A. Scarmi, G.D. Soraru', R. Raj, J. Non-Cryst. Solids 351 (2005) 2238–2243.
[7] T. Rouxel, G.D. Sorarù, J. Vicens, J. Am. Ceram. Soc. 84 (2001) 1052–1058.
[8] L. Ferraioli, D. Ahn, A. Saha, L. Pavesi, R. Raj, J. Am. Ceram. Soc. 91 (2008) 2422–2424.
[9] A. Karakuscu, R. Guider, L. Pavesi, G.D. Sorarù, J. Am. Ceram. Soc 92 (2009) 2969–2974.
[10] I. Menapace, G. Mera, R. Riedel, E. Erdem, R.-A. Eichel, A. Pauletti, G.A. Appleby, J. Mater. Sci. 43 (2008) 5790–5796.
[11] H.–Y. Ryu, Q. Wang, R. Raj, J. Am. Ceram. Soc., in press.
[12] C. Haluschka, C. Engel, R. Riedel, J. Eur. Ceram. Soc. 20 (2000) 1365–1374.
[13] L. Zhang, Y. Wang, Y. Wei, W. Xu, D. Fang, L. Zhai, K.C. Lin, L. An, J. Am. Ceram. Soc. 91 (2008) 1346–1349.
[14] Terauds, P. E. Jimenez–Sanchez, R. Raj, C. Vakifahmetoglu, P. Colombo, J. Eur. Ceram. Soc., in press.
[15] W.B. Xing, A.M. Wilson, K. Eguchi, G. Zank, J.R. Dahn, J. Electrochem. Soc. 144 (1997) 2410–2416.
[16] P. E. Sanchez–Jiminez, R. Raj, J. Am. Ceram. Soc., in press.
[17] D. Ahn and R. Raj, submitted for publication.
[18] W. Weppner, R.A. Huggins, J. Electrochem. Soc. 124 (1997) 1569–1578.
[19] Y.S. Jung, A.S. Cavanagh, A.C. Dillon, M.D. Groner, S.M. George, S. Lee, J. Electrochem. Soc. 157 (2010) A75–A81.
[20] S.M. George, Chem. Rev. 110 (2010) 111–131.
[21] T. Zheng, W.R. McKinnon, J.R. Dahn, J. Electrochem. Soc. 143 (1996) 2137–2145.
[22] M. Inaba, M. Fujikawa, T. Abe, Z. Ogumi, J. Electrochem. Soc. 147 (2000) 4008–4012.